Cancer Chemother Pharmacol (2003) 52: 25–33
DOI 10.1007/s00280-003-0621-0

ORIGINAL ARTICLE

**Ramesh R. Boinpally · Lisa Polin · Sen-Lin Zhou
Bhaskara R. Jasti · Richard A. Wiegand · Kathryn White
Juiwanna Kushner · Jerome P. Horwitz
Thomas H. Corbett · Ralph E. Parchment**

Pharmacokinetics and tissue distribution of cryptophycin 52 (C-52) epoxide and cryptophycin 55 (C-55) chlorohydrin in mice with subcutaneous tumors

Received: 20 November 2002 / Accepted: 11 March 2003 / Published online: 9 May 2003
© Springer-Verlag 2003

Abstract *Purpose*: To compare the pharmacokinetics and tissue distribution (both normal and tumor) of cryptophycin 52 (C-52) and its putative chlorohydrin prodrug cryptophycin 55 (C-55) in a murine model and to investigate a possible mechanism behind the superior activity of C-55. *Methods*: Mammary adenocarcinoma 16/c tumor-bearing mice were treated with an i.v. bolus of 11 mg/kg C-52 or 38 mg/kg C-55 in Cremophor-alcohol. At predetermined time intervals, C-52 and C-55 concentrations in plasma, liver, kidney, small intestine and tumors were measured using a previously described HPLC method. Pharmacokinetic parameters were computed using noncompartmental methods. Tissue (both normal and tumor) to plasma ratios as a function of time were also calculated for comparison. *Results*: Both C-52 and C-55 were rapidly distributed into different tissues including tumors following i.v. administration. However, the affinities of these compounds towards different tissues were different. Thus, the half-lives (minutes) of C-55 were in the decreasing order liver (725), intestine (494), tumor (206), kidney (62) and plasma (44), whereas the AUC values (μg·min/ml) were in the order tumor (9077), liver (7734), kidney (6790), plasma (2372) and intestine (2234). For C-52, the half-lives (minutes) were in the decreasing order liver (1333), kidney (718), intestine (389), tumor (181) and plasma (35), and the AUC values (μg·min/ml) were in the order kidney (1164), liver (609), intestine (487), plasma (457) and tumor (442). The relative exposures to C-52 after i.v. injection of C-55 were plasma 3.9%, tumor 80.8%, kidney 3.4%, liver 1.1% and intestine 2.8%. Although plasma exposure to C-52 following C-55 administration was relatively small, the use of C-55 to deliver C-52 increased the retention of C-52 and its AUC in tumor compared to direct injection of C-52. Simultaneously, this approach shortened C-52 retention in all normal tissues studied. *Conclusions*: The distribution of C-55 and its bioconversion to C-52 in different organs and tumor tissue observed in this study suggest the ability of C-55 to target tumor tissue, creating a depot of C-52 in tumor. Increased C-52 exposure of tumor, with concomitant decreased exposure of normal tissue, is a contributing factor to the superior activity of C-55 versus C-52. However, except in the case of tumor tissue in which 81% of C-55 converts to C-52, only a minor amount of C-55 may serve as a prodrug for C-52, whereas the majority is handled by the biosystem through a different route of elimination. Tissue distribution combined with rate of conversion may be an important determinant of the relative effectiveness of other epoxide-chlorohydrin pairs of cryptophycins.

Keywords Natural product · Clearance · Exposure · Therapeutic index · Disposition · Prodrugs

R. R. Boinpally (✉) · L. Polin · S.-L. Zhou · B. R. Jasti
R. A. Wiegand · K. White · J. Kushner · J. P. Horwitz
T. H. Corbett · R. E. Parchment
The Barbara Ann Karmanos Cancer Institute,
Wayne State University, Detroit,
MI 48201, USA
E-mail: parchmen@med.wayne.edu
Tel.: +1-313-9667327
Fax: +1-313-9667322

R. E. Parchment
HWCRC-523, 110 E. Warren,
Detroit, MI 48201, USA

Present address: B. R. Jasti
Thomas J. Long School of Pharmacy,
University of the Pacific,
Stockton, CA, USA

Introduction

Cryptophycins are a class of antitubulin antitumor agents [1, 2, 3]. The antimitotic activity, cytotoxicity toward tumor cells in vitro, and anticancer activity

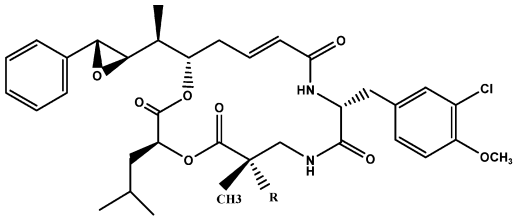

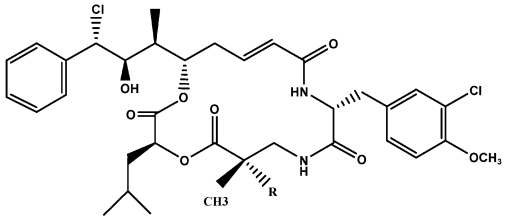

Fig. 1 Structures of the cryptophycin epoxides, cryptophycin-1 and cryptophycin-52, and chlorohydrins, cryptophycin-8 and cryptophycin-55

against murine solid tumor models and human tumor xenografts of cryptophycin-1 (C-1), a desipeptide isolated from the cyanobacterium *Nostoc* species, prompted the isolation and synthesis of several cryptophycins [4, 5, 6, 7, 8, 9, 10, 11]. Early in this analog synthesis effort it was found that the conversion of the epoxide of C-1 to its chlorohydrin called cryptophycin-8 (C-8, Fig. 1) markedly improved efficacy [1, 2]. Although potentially a promising clinical candidate, C-8 had an asymmetric center, which made bulk synthesis difficult. Thus, further synthetic effort eliminated this center, creating the pair C-52 (the epoxide) and C-55 (the chlorohydrin) (for structures see Fig. 1). Like the C-1/C-8 pair, the C-55 chlorohydrin is markedly more active in tumor-bearing mice than the C-52 epoxide (Tables 1 and 2) [3, 12, 13]. Often, C-55 exhibits 10- to 100-fold higher cell kill than C-52 at equimolar dosing, resulting in curative activity that is rarely observed with C-52 (Tables 1 and 2).

This remarkable difference in efficacy observed with both chlorohydrin-epoxide pairs resulting from a small structural change suggests an underlying mechanism for this superior activity. Since the chemical structure of C-55 suggests that it will convert into the C-52 epoxide, we undertook a comparative study of the pharmacokinetics and tumor/normal tissue distribution of intravenously administered C-52 and C-55, and C-52 formed from C-55 in vivo to find out if differences in drug disposition explain these large differences in efficacy. The doses of C-52 and C-55 used in this study were the daily doses from the optimal dosage regimen (equally well tolerated) used in the evaluation of antitumor activity for the mammary 16/c tumor model (Table 1).

Table 1 Comparison of C-52 with C-55 against solid tumors of mouse and human origin. C-55 (the chlorohydrin) was markedly more active than C-52 (the epoxide) in most tumor models. The optimum dose schedules used were not the same for all trials. An optimum dose schedule was used for each individual comparison. The strain of mice used can affect dose schedule. The host of origin is specific to each tumor model, so some strains were more resilient to chemotherapy than others. Tumor biology also can have an effect on the optimum dose schedule: tumors with a faster doubling time may require a different, more aggressive schedule than tumors growing more slowly. Details about dosage regimens can be found in references 1 and 2

Tumor	Origin	Stage	C-52 (optimum dose schedule)						C-55 (optimum dose schedule)					
			T/C (%)	Regression		Log cell kill	Cures	Activity rating[a]	T/C (%)	Regression		Log cell kill	Cures	Activity rating[a]
				Partial	Complete					Partial	Complete			
TSU prostate	Human	Advanced	15	0/5	0/5	1.8	0/5	+ +	0	5/5	5/5	4.0	2/5	+ + + +
LNCaP prostate	Human	Advanced	7	5/5	1/5	3.2	0/5	+ + + +	0	5/5	5/5	5.9	3/5	+ + + +
PC-3 prostate	Human	Advanced	32	4/5	2/5	0.4	0/5	+	0	4/5	4/5	2.9	0/5	+ + + +
H116 colon	Human	Advanced	4	2/5	0/5	2.4	0/5	+ + +	8	4/5	3/5	3.6	0/5	+ + + +
H125 lung	Human	Early	5			1.8	0/5	+ +	0			2.4	0/5	+ + +
WSU pancreas	Human	Early	16			1.0	0/5	+	4			2.4	0/5	+ + +
Panc 03		Early	3			1.9	0/5	+ +	0			> 4.5	5/5	+ + + +
Colon 38		Advanced	9	4/5	0/5	3.3	0/5	+ + + +	15	5/5	2/5	4.2	2/5	+ + + +
Mam 16/C		Early	5			1.2	1/5	+ +	0			3.9	0/5	+ + + +
Mam 16/C/Adr		Early	2			2.0	0/5	+ + +	0			2.4	0/5	+ + +
Mam 17/Adr		Early	10			1.6	0/5	+ + +	0			2.1	0/5	+ + +
Panc 02		Early	9			2.3	0/5	+ + +	9			2.9	0/5	+ + + +
Colon 26		Early	14			1.1	0/5	+	0			1.2	0/5	+

[a]The activity rating system did not specifically delineate curative potential from high activity (> 2.8 log kill)

Table 2 Comparison of the activities of cryptophycin epoxide and chlorohydrin analogs [3]

Model	Efficacy measure	Treatment	Epoxide	Chlorohydrin
In vitro				
H460 human NSCLC	Bcl-2 phosphorylation	C-52/C-55, 4 h	0.05 n*M*	0.25 n*M*
	IC_{90}	C-52/C-55, 24 h	0.13 n*M*	0.20 n*M*
Calu-6 human NSCLC	IC_{90}	C-52/C-55, 24 h	0.03 n*M*	0.10 n*M*
In vivo				
MX-1 human breast carcinoma	Tumor growth delay	C-52/C-55 i.v.	11.4 days	18.8 days
SW2 human SCLC	Tumor growth delay	C-52/C-55 i.v.	6.8 days	8.7 days
H82 human SCLC	Tumor growth delay	C-52/C-55 i.v.	12.7 days	20.9 days
H460 human NSCLC	Tumor growth delay	C-52/C-55 i.v.	11.3 days	16.0 days
Calu-6 human NSCLC	Tumor growth delay	C-52/C-55 i.v.	14.9 days	16.6 days
13762 rat mammary carcinoma	Tumor growth delay	C-52/C-55 6-h infusion	8.5 days	11 days
		C-292/C-296 6-h infusion	17 days	10 days

Material and methods

In vivo chemotherapy

The protocol design, drug treatment, toxicity evaluation, data analysis, quantification of tumor cell kill, tumor model systems, and the biological significance of the drug treatment results with transplantable tumors have been presented previously [1, 2, 7, 14, 15]. The methods as they apply to this work are described briefly in the following sections.

Tumor maintenance

Tumors were maintained in the mouse strain of origin and were transplanted into the appropriate F_1 hybrid or inbred for the chemotherapy trials. Human tumors were maintained in Balb/c-SCID or ICR-SCID mice. Individual mouse body weights for each experiment were within 5 g, and all mice were over 18 g at the start of therapy. The mice were supplied with food and water ad libitum.

Chemotherapy of solid tumors

The animals were pooled, implanted bilaterally subcutaneously with 30 to 60 mg of tumor fragments using a 12-gauge trocar, and again pooled before unselective distribution to the various treatment and control groups. For early-stage treatment, chemotherapy was started within 1 to 3 days after tumor implantation, when the number of cells was relatively small (10^7 to 10^8 cells). For treatment during more advanced stages, the tumors were allowed to become palpable (120 to 400 mg) before the first treatment. Tumors were measured with a caliper twice or three times weekly (depending on the doubling time of the tumor). Mice were killed when their tumors reached 1500 mg. Tumor weights were estimated from two-dimensional measurements, i.e., tumor weight in milligrams = $(a \times b^2)/2$, where a and b are the tumor length and width in millimeters, respectively. For the calculation of end-points, both tumors on each mouse were added together, and the total mass per mouse was used.

End-points for assessing antitumor activity for solid tumors

Tumor growth delay This is expressed as the T–C value where T is the median time (in days) required for the treatment group tumors to reach a predetermined size (e.g., 1000 mg), and C is the median time (in days) for the control group tumors to reach the same size. Tumor-free survivors were excluded from these calculations (cures are tabulated separately). In our judgment, this value is the single most important criterion of antitumor effectiveness because it allows the quantification of tumor cell kill.

Table 3 Activity rating

Antitumor activity		Gross $\log_{10}$ tumor cell kill[a]
Highly active	+ + + +	> 2.8
	+ + +	2.0–2.8
	+ +	1.3–1.9
	+	0.7–1.2
Inactive	–	< 0.7

[a]Duration of treatment 5–20 days

Regressions (advanced stage primary tumors) Complete regression (CR) was considered to be regression below the limit of palpation (< 60 mg). Partial regression (PR) was considered to be a greater than 50% reduction in tumor mass. CRs are included in the tabulation of PRs. Cures are included in the tabulation of PRs and CRs.

Calculation of tumor cell kill For subcutaneously growing tumors, the $\log_{10}$ cell kill was calculated from the following formula:

$$\text{The } \text{Log}_{10} \text{ Cell Kill Total (gross)} = \frac{\text{T} - \text{C value in days}}{(3.32)\ (\text{Td})}$$

where T–C is the tumor growth delay as described above and Td is the tumor volume doubling time (in days), estimated from the best fit straight line from a log-linear growth plot of the control group tumors in exponential growth (100 to 800 mg range). The conversion of the T–C values to $\log_{10}$ cell kill is possible because the Td of tumors regrowing posttreatment approximates the Td value of tumors in untreated control mice.

Activity rating For comparison of activity with standard agents and comparison of activity between tumors, the $\log_{10}$ kill values were converted to an arbitrary activity rating (Table 3) [2, 7, 15].

Nonquantitative determination of antitumor activity by tumor growth inhibition (T/C value) The treatment and control groups were measured when the control group tumors reached a median weight of approximately 700 to 1200 mg. The median tumor weight of each group was determined (including zeros). The T/C value in percent is an indication of antitumor effectiveness. A T/C value equal to or less than 42% is considered to indicate significant antitumor activity by the Drug Evaluation Branch of the Division of Cancer Treatment (NCI). A T/C value < 10% is considered to indicate highly significant antitumor activity, and is the level used by the NCI to justify a clinical trial if toxicity, formulation, and certain other requirements are met (termed DN-2 level activity). A mean body weight loss nadir of greater than 20% or greater than 20% drug-related deaths is considered to indicate an excessively toxic dosage.

Animals and tumor implantation for pharmacokinetic and tissue distribution studies

These studies were performed under a protocol approved by the Wayne State University IACUC. C3H female mice of mean body weight 20 g (range 18.7–22 g) were pooled, implanted bilaterally subcutaneously with 30 to 60 mg fragments of mammary adenocarcinoma 16/c using a 12-gauge trocar on day 0 and again pooled before unselective distribution to the various groups, each of which comprised three mice. The tumors were allowed to grow for 7 days before i.v. injection of the cryptophycins.

Drug preparations

Both C-52 and C-55 formulations were prepared in Cremophor (5.5%), alcohol (5.5%) and warm distilled water (89%) from stock solutions in 50% each of ethanol and Cremophor such that 0.2 ml contained the required dose. C-52 preparations sufficient for each group of three animals were prepared 2 min prior to administration, whereas C-55 preparations required for all animals on a single day were prepared and used within 45 min.

Drug disposition study

The sampling points were chosen based on the pharmacokinetic data from a pilot study conducted in nine mice at three time-points prior to this study. Longer time-points were not possible because a single dose at the daily maximal tolerated dose of a multiday regimen is not sufficient to substantially delay tumor growth.

C-52 study

A total of 42 mice bearing bilateral tumors (average mass 743 mg, range 283–953 mg) were divided into 14 groups at random with three animals in each group. One group served as a control and was treated with vehicle (Cremophor-alcohol). Each animal in the remaining 13 groups was injected i.v. with 11 mg/kg C-52. The animals were anesthetized for 2 min in CO_2 starting 2 min prior to each scheduled time-point at 5, 6, 7, 10, 15, 27, 28, 48, 64, 120, 360, 1440 and 1740 min after injection. Blood was collected by intracardiac puncture into a 1-ml tuberculin syringe preloaded with 0.1 ml heparin sodium USP, microfuged for 5 min at 14,000 *g* at room temperature, and the plasma fraction was separated, weighed and immediately frozen. The dilution factor was calculated from the total volume of heparinized plasma recovered. Unconscious animals were killed by cervical dislocation. Kidney, liver and tumor were harvested into individual preweighed tubes and quick-frozen in a dry-ice bath. Small intestine was flushed with 5 ml ice-cold saline to expel residual luminal contents, and then frozen. All the samples were frozen at −80°C until assay.

C-55 study

A total of 42 mice bearing bilateral tumors (average mass 1644 mg, range 853–2578 mg) were divided into 14 groups at random with three animals in each group. One group served as a control and was treated with vehicle (Cremophor-alcohol). Each animal in the remaining 13 groups was injected i.v. with 38 mg/kg C-55. The animals were anesthetized and subsequently killed as described above at 2, 5, 7, 10, 15, 30, 45, 60, 120, 360, 1440, 1740 and 2880 min after injection. Plasma and the different tissues were harvested and stored at −80°C until C-52 and C-55 were assayed.

Assay

C-52 and C-55 in the biological samples were quantified using a reversed-phase HPLC method. The method of Foster et al. [16] for the analysis of cryptophycin 1 was modified to quantify C-52 and C-55 in this study. A known volume of frozen heparinized plasma (weighed at the time of storage) was thawed under an equal volume of acetonitrile, mixed thoroughly by vortex, microfuged at 4°C for 10 min and the supernatant was analyzed by HPLC. Concentrations were corrected for the dilution with the 0.1 ml heparin used as anticoagulant; any samples diluted greater than tenfold were excluded from analysis. Frozen tissue (liver, kidney, tumor, intestine) was homogenized in 1 ml calcium and magnesium-free saline per gram of frozen wet tissue by ten 5-s strokes of a Polytron PT 2100 homogenizer fitted with a Polytron PT-DA 2112/2EC probe. An equal volume of acetonitrile was added, the contents mixed thoroughly by vortexing five times, and a clarified supernatant prepared for HPLC analysis by microfuging for 10 min at 4°C.

HPLC conditions

Two Waters Nova-Pak C18 4 μm (3.9×150 mm) columns in series maintained at 28°C were used in the analysis. The mobile phase was 60% acetonitrile in water at a flow rate of 1.0 ml/min and the analytes were detected at 220 nm. Tissue homogenates and plasma from vehicle-treated (control) animals were analyzed to prove lack of interfering peaks. Some of these, as well as some drug-containing samples, were spiked with standards after initial analysis to confirm

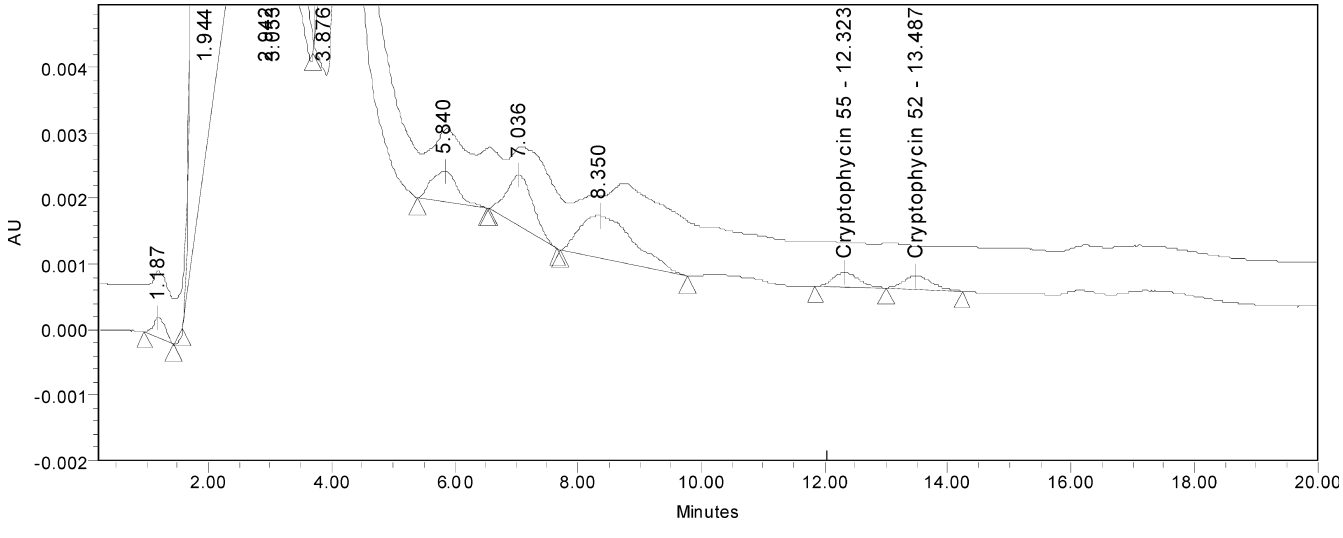

Fig. 2 Overlay of chromatograms from blank plasma and plasma spiked with 0.025 μg/ml C-52 and C-55. Note the clear separation of the cryptophycins

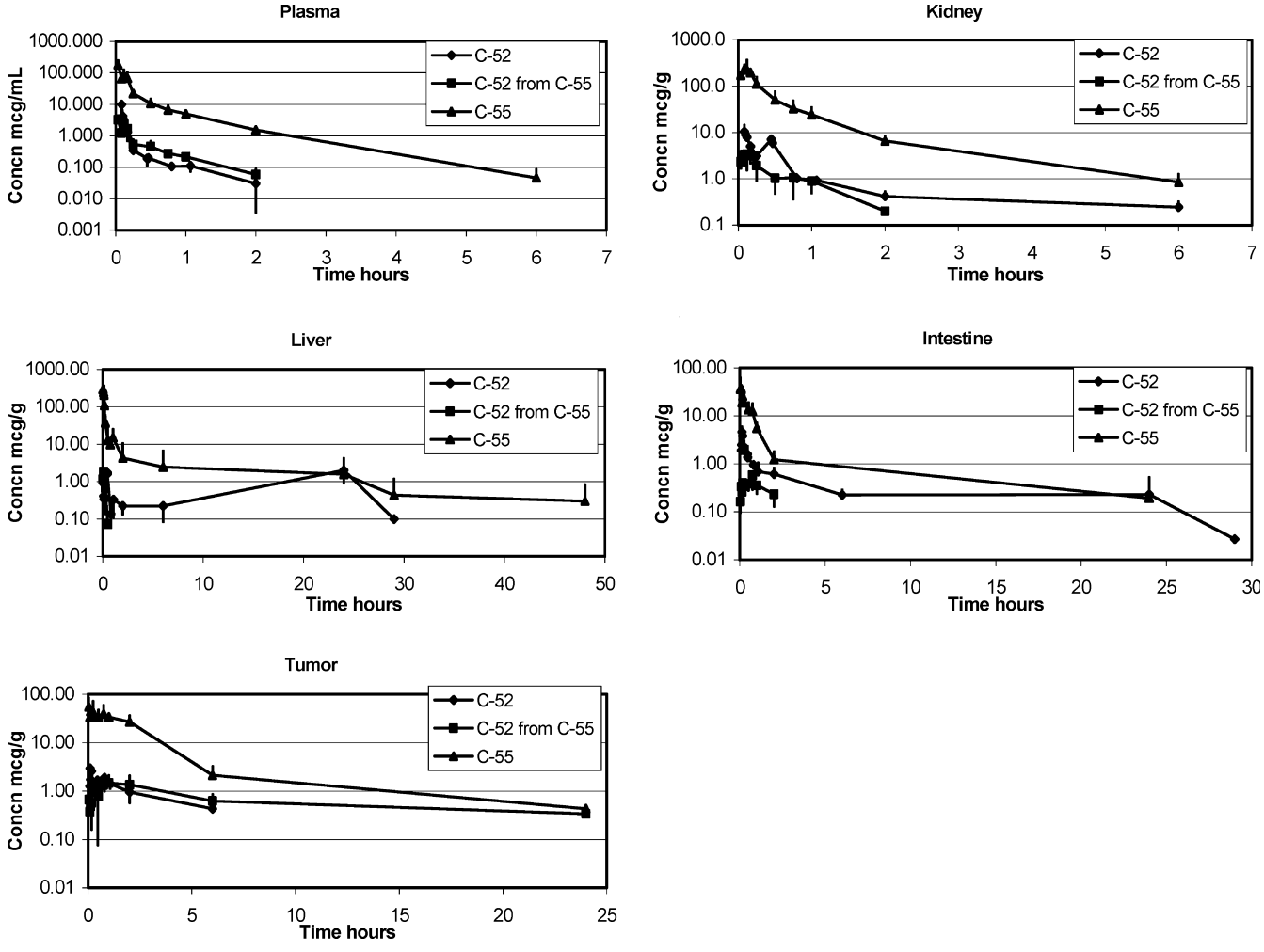

Fig. 3 Time-course of C-52, C-55 and C-52 from C-55 concentrations in plasma, kidney, liver, intestine and tumor following i.v. injections of C-52 and C-55. Note differences in the concentration range (y-axis) and the time frame (x-axis) for each panel, which was determined by the earliest time-point at which drug levels reached undetectable levels in the particular tissue

the analyte peaks by coelution with standards. The retention times for C-52 and C-55 were 13.5 and 12.3 min, respectively. An overlay of chromatograms from blank plasma along with blank plasma spiked with 0.025 μg/ml of each cryptophycin is shown in Fig. 2. Linearity was obtained in the range of 0.025–250 μg/ml for both C-52 and C-55 ($r^2 > 0.99$) with an intra-/interday coefficient of variation $< 8\%$. There were no differences in standard curve peak areas of standards from neat samples versus spiked tissue homogenates from vehicle-treated animals, indicating complete analyte recovery.

Pharmacokinetic analysis

Pharmacokinetic parameters of C-52 and C-55 were computed from the mean plasma concentration-time data employing non-compartmental methods using WinNonlin 3.1 (Pharsight, Mountain View, Calif.). Further, the extent of biotransformation of C-55 to C-52 was calculated employing the following equation [17]:

$$\mathrm{Fm} = \frac{\text{dose(metabolite)X AUCm (parent given; 0, } \infty)}{\text{dose (parent) X AUCm (metabolite given; 0, } \infty)}$$

Results

The time-courses of mean plasma and tissue concentrations of C-52 and C-55 following single-dose i.v. injections of the respective agents are shown in Fig. 3 and the corresponding pharmacokinetic parameters are listed in Table 4. Plasma concentrations of C-55 following its i.v. injection exhibited a biexponential decline with a rapid distribution phase followed by slow elimination phase. C-55 was rapidly distributed into kidney, liver, intestine and tumor tissue. However, the C-55 levels (per gram weight) in different organs varied, indicating that the agent has different affinities for different organs. No C-55 was detectable in plasma at 24 h. Except at the 2-min time-point in kidney, the mean C-55 levels in kidney and liver were much higher than in plasma at all time-points. The organ/plasma ratios of C-55 shown in Fig. 4 reveal this. Interestingly, C-55 was found in liver even at 48 h, although it was not detectable after 6 h in plasma. The pharmacokinetic parameters AUCs and half-lives listed in Table 4 further substantiate these observations. The half-lives of C-55 were in the decreasing order liver > intestine > tumor >

Table 4 Pharmacokinetic parameters of C-52 and C-55 in mice following their i.v. bolus injection at 11 mg/kg and 38 mg/kg, respectively

Parameter	Plasma			Kidney			Liver			Intestine			Tumor		
	C-55	C-52	C-52 from C-55	C-55	C-52	C-52 from C-55	C-55	C-52	C-52 from C-55	C-55	C-52	C-52 from C-55	C-55	C-52	C-52 from C-55
C_{max} (μg/ml)	359.22	157.60	6.13	235.03	10.43	3.41	296.34	2.02	1.88	36.32	4.63	0.58	55.05	2.96	1.48
AUC_{0-t} (μg·min/ml)	2368.72	455.17	62.14	6714.50	911.78	125.87	7418.20	418.81	22.91	2096.60	472.30	38.12	8949.40	329.00	900.10
$AUC_{0-\infty}$ (μg·min/ml)	2371.66	456.69	62.19	6789.82	1163.50	134.70	7734.20	609.13	23.42	2234.10	487.40	47.46	9077.40	441.80	1232.90
$t_{1/2}$ (min)	44.30	35.11	39.00	62.10	718.02	30.40	725.40	1332.51	4.85	493.80	389.20	41.80	206.40	181.40	682.50
V_z (ml)	25.61	30.50		12.52	244.84		128.50	867.89		302.90	316.80		31.20	162.90	
Cl (ml/min)	0.40	0.60		0.14	0.24		0.12	0.45		0.43	0.56		0.11	0.62	

kidney > plasma, whereas the AUCs were in the order tumor > liver > kidney > plasma > intestine.

C-55 levels in kidney increased up to 5 min and then declined in a biexponential fashion, indicating that the agent is not instantaneously distributed into this organ and it does not fall into the central compartment. In contrast, C-55 appears to instantaneously distribute to liver and intestine in which the drug levels were maximum at 2 min and declined subsequently. Unlike in plasma, kidney and liver, there was no appreciable change in C-55 levels in tumor up to 1.5–2 h, followed by a rapid decline.

The mean plasma concentrations of C-52 following its i.v. bolus injection exhibited a biexponential decay with a rapid distribution and a slow elimination phase. The agent was detected up to 2 h in plasma. C-52 was rapidly distributed to kidney and the levels were higher when compared to plasma concentrations at all time-points. The drug was detected in kidney up to 24 h. Unlike in kidney, the C-52 levels increased initially and then declined in liver, intestine and tumor. Secondary peaks at about 30 min were observed in kidney and liver. The half-lives of C-52 in different tissues were in the decreasing order liver > kidney > intestines > tumor > plasma, and the AUCs were in the order kidney > liver > intestine > plasma > tumor.

The organ/plasma ratios of C-52 are shown in Fig. 4. The kidney/plasma ratio of C-52 increased rapidly up to 30 min and then rapidly declined. However, the ratios were greater than 1 at all time-points. Interestingly, the C-52 tumor/plasma ratio increased almost steadily until the end, indicating the persistence of this agent in tumor despite its rapid clearance from the systemic circulation. However, tumor C-52 fell to undetectable levels after 6 h.

The mean plasma or tissue concentration-time profiles of C-52 following C-55 injection are shown in Fig. 3. C-52 concentration in plasma was highest at the first sampling point of 2 min, indicating that C-55 is rapidly converted to C-52 following its injection. However, the relative conversion of C-55 to C-52 and the relative clearance of the latter appeared to be 3.94%. C-52 concentrations increased up to 7 min and 5 min in kidney and liver, respectively, following C-55 injection and declined thereafter. It is important to note that the C-52 concentrations in tumor increased steadily and remained high even at 24 h after injection. Although systemic availability of C-52 following C-55 injection was much less compared to that following direct injection of C-52, the AUC_{0-t} and $AUC_{0-\infty}$ of C-52 in tumor were threefold higher following C-55 than C-52 injections (Table 4). The half-lives of C-52 after C-55 injection in different tissues were in the decreasing order tumor > > intestine > plasma > kidney > liver and the AUCs were in the order tumor > kidney > plasma > intestine > liver. This rank order of half-lives was very different from the rank order of half-lives following injection of C-52 directly. Relative exposures of different tissues/organs to C-52 after the i.v. injection of C-55

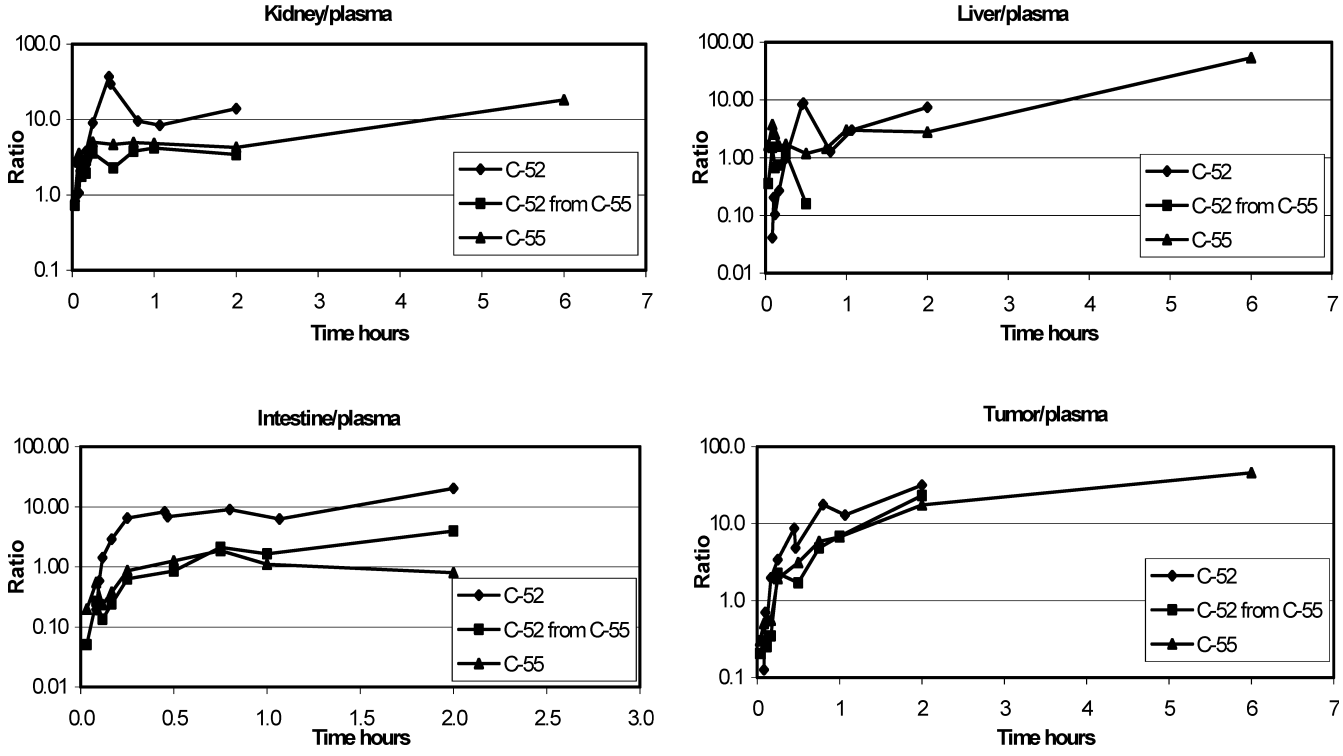

Fig. 4 Time-course of organ/plasma ratios of C-52, C-55 and C-52 from C-55 in kidney, liver, intestine and tumor following i.v. injections of C-52 and C-55

were: plasma 3.9%, tumor 80.8%, kidney 3.4%, liver 1.1% and intestine 2.8%.

Discussion

Selective distribution of antitumor agents to tumor tissue while sparing the non-target tissues is of paramount importance in determining efficacy and toxicity. In this study, the pharmacokinetics and distribution of C-52 and C-55 were investigated in mice following their i.v. injection. Further, whether C-55 can serve as a prodrug to C-52, and why C-55 is more effective than C-52, were addressed by studying the pharmacokinetics and tissue distribution of C-52 after C-55 injection.

The biexponential decay of C-52 as well as C-55 plasma levels following their i.v. injection revealed that the drugs were rapidly distributed into different tissues, although at different rates, and there exists a central as well as a peripheral compartment for the distribution of both these agents. It is important to note that, despite very high plasma protein binding (99% to albumin) of C-52 [18], the drug was rapidly distributed and cleared from plasma. This could have been because of greater affinities or higher association constants for C-52 with the different tissue proteins compared to plasma. Selective affinity of C-52 for human high-density lipoprotein (HDL) and low-density lipoprotein, but not for murine HDL, has been reported [19].

Both C-52 and C-55 are rapidly cleared from plasma and had similar terminal elimination half-lives (35 min for C-52 and 44 min for C-55, Table 4). However, the affinities/retention times of C-52 and C-55 to different organs were different. C-52 was retained in kidney for a very long time with a terminal half-life of 718 min following its direct administration at a relatively high dose (11 mg/kg) in contrast to when it was formed from the conversion of C-55 to C-52. The half-life in the latter case was 30 min, where only 3.4% of the C-55 dose of 38 mg/kg appeared to be converted to C-52, i.e., about 1.27 mg/kg of C-52. This indicates dose-dependent elimination of C-52 from kidney and the potential for organ toxicity at higher doses or with prolonged administration.

In liver, the half-life of C-52 was almost double that of C-55 and once again the half-life of C-52 was much shorter following C-55 administration, clearly indicating that the enzyme system(s)/pathway(s) responsible for the elimination of C-52 are saturated at higher doses. The conversion of C-55 to C-52 appeared to be much less (1.1%) in liver than in other organs. In intestine, C-55 exhibited a slightly longer half-life than C-52 (494 versus 389 min) and once again the half-life of C-52 in intestine following C-55 dosing was much shorter, indicating dose-dependent elimination of C-52 from this organ as well.

In tumor, C-55 had a longer half-life than C-52 (206 versus 181 min). In contrast to the findings in normal tissues, the half-life of C-52 after C-55 administration was very much prolonged in tumor tissue (683 min), revealing that conversion of C-55 to C-52 governs the C-52 retention in this tissue. Since C-55 levels remained

high in tumor tissue, C-52 levels were also correspondingly high as 81% of C-55 was converted to C-52 in this tissue. The prolonged maintenance of C-52 levels in tumor also depends on adequate C-55 conversion, because, unlike in tumor, prolonged high C-55 levels in liver did not result in long-term C-52 exposure in that tissue.

The potential of cryptophycins as antitumor agents is well recognized, and the C-52 epoxide is currently in clinical evaluation. However, our study showed that tissue distribution might be an important determinant in the relative effectiveness of epoxide–chlorohydrin pairs of cryptophycin analogs. The distribution of C-55 and its bioconversion to C-52 in different organs and tumor tissue observed in this study suggest the ability of C-55 to target tumor tissue and to serve as a depot of C-52 in tumor. In combination with the prolonged conversion of C-55 into C-52 observed in tumor but not liver, note that the relative retention of C-52 following its direct administration versus following C-55 injection shows exactly opposite features in normal tissues and tumor tissue. C-52 retention in tumor was increased 3.5-fold with a corresponding 3-fold increase in AUC by producing C-52 from C-55, rather than directly injecting C-52. At the same time, using C-55 to deliver systemic C-52 shortened C-52 retention in all normal tissues studied by at least 10-fold.

In addition, the much shorter half-lives of C-55 in kidney and liver when compared to C-52 also contribute to its relative safety over C-52. However, the much shorter half-lives of C-52 following C-55 administration reveal that only a minor amount of C-55 may serve as a prodrug for C-52, whereas the majority is eliminated through a different route. This gain in tumor exposure while substantially decreasing exposure of normal tissue would be expected to be an important reason for the superior activity of C-55 in the mammary 16/c tumor model. Furthermore, the general finding that C-55 is superior to C-52 in all murine and human tumor models suggests that selective tumor uptake and conversion is generalizable to many tumor types (Tables 1 and 2). However, the principle that chlorohydrins are intrinsically superior to epoxides is not generalizable, as the comparison of C-292 and C-296 illustrates (Table 2). A comparative study of the pharmacokinetics and distribution of the C-1/C-8 and C-292/C-296 pairs similar to the one in this report might reveal interesting and important information about epoxide conversion in the tumor microenvironment.

Shih and Teicher [3] have recently reviewed the antitumor activities of cryptophycins, and the information on C-52 and C-55 in their article and our own data are summarized in Tables 1 and 2. C-52 appears to be superior to C-55 in vitro. However, in all the in vivo models (rat mammary carcinoma and human tumor xenografts) tested, C-55 was significantly more active than C-52, both when tested as single agents and when used in combination regimens. The results of the present study suggest two possibilities for the higher in vivo efficacy of C-55. In the event that C-55 itself is eliciting pharmacological activity, accumulation of C-55 in tumor in higher concentrations for prolonged periods might contribute to better activity. In the second scenario wherein C-55's activity is through conversion to C-52, C-55 serves as a depot of C-52 resulting in selective, prolonged exposure of tumor to C-52 and better activity. Incubation of C-55 in FBS-containing cell culture medium of pH 7.4 at 37°C and quantification of both C-55 and C-52 as a function of time has revealed conversion of more than 50% of C-55 to C-52 in 24 h (unpublished data). So, enzyme involvement is not necessarily required for conversion, and it appears that even the in vitro activity of C-55 could be due to the C-52 generated in cells or culture medium upon incubation. Furthermore, the extracellular pH in tumor is reported to be typically lower, while the intracellular pH is equal to that in normal tissue or slightly more alkaline [20]. Although we have not tested the stability of C-55 in acidic medium, perhaps the lower pH of the extracellular fluid in tumor might stabilize C-55, thus prolonging its half-life. The alkaline intracellular pH should favor conversion of C-55 to C-52 to elicit pharmacological activity.

Acknowledgements We acknowledge the expert technical support by Joseph Kassab and Andrew Erickson, and assistance by Daniel Black. Supported by NIH grants U19-CA53001 and U01-CA62487.

References

1. Corbett TH, Valeriote FA, Demchik L, Lowichik N, Polin L, Panchapor C, Pugh S, White K, Kushner J, Rake J, Wentland M, Golakoti T, Hetzel C, Ogino J, Patterson G, Moore R (1997) Discovery of cryptophycin-1 and BCN-183577: examples of strategies and problems in the detection of antitumor activity in mice. Invest New Drugs 15:207–218
2. Corbett TH, Valeriote FA, Demchik L, Polin L, Panchapor C, Pugh S, White K, Knight J, Jones J, Jones L, LoRusso P, Foster B, Wiegand RA, Lisow L, Golakoti T, Heltzel CE, Ogino J, Patterson GM, Moore RE (1996) Preclinical anticancer activity of cryptophycin-8. J Exp Ther Oncol 1:95–108
3. Shih C, Teicher BA (2001) Cryptophycins: a novel class of potent antimitotic antitumor depsipeptides. Curr Pharm Des 7:1259–1276
4. Panda D, Himes RH, Moore RE, Wilson L, Jordan MA (1997) Mechanism of action of the unusually potent microtubule inhibitor cryptophycin 1. Biochemistry 36:12948–12953
5. Panda D, DeLuca K, Williams D, Jordan MA, Wilson L (1998) Antiproliferative mechanism of action of cryptophycin-52: kinetic stabilization of microtubule dynamics by high-affinity binding to microtubule ends. Proc Natl Acad Sci U S A 95:9313–9318
6. Panda D, Ananthnarayan V, Larson G, Shih C, Jordan MA, Wilson L (2000) Interaction of the antitumor compound cryptophycin-52 with tubulin. Biochemistry 39:14121–14127
7. Polin L, Valeriote F, White K, Panchapor C, Pugh S, Knight J, LoRusso P, Hussain M, Liversidge E, Peltier N, Golakoti T, Patterson G, Moore R, Corbett TH (1997) Treatment of human prostate tumors PC-3 and TSU-PR1 with standard and investigational agents in SCID mice. Invest New Drugs 15:99–108
8. Smith AB 3rd, Cho YS, Zawacki LE, Hirschmann R, Pettit GR (2001) First generation design, synthesis, and evaluation of azepine-based cryptophycin analogues. Org Lett 3:4063–4066

9. Shih C, Gossett LS, Gruber JM, Grossman CS, Andis SL, Schultz RM, Worzalla JF, Corbett TH, Metz JT (1999) Synthesis and biological evaluation of novel cryptophycin analogs with modification in the beta-alanine region. Bioorg Med Chem Lett 9:69–74
10. Varie DL, Shih C, Hay DA, Andis SL, Corbett TH, Gossett LS, Janisse SK, Martinelli MJ, Moher ED, Schultz RM, Toth JE (1999) Synthesis and biological evaluation of cryptophycin analogs with substitution at C-6 (fragment C region). Bioorg Med Chem Lett 9:369–374
11. Subbaraju GV, Golakoti T, Patterson GM, Moore RE (1997) Three new cryptophycins from *Nostoc* sp. GSV 224. J Nat Prod 60:302–305
12. Corbett T, Valeriote F, Moore R, Tius M, Barrow R, Hemscheidt T, Liang J, Paik S, Polin L, Pugh S, Kushner J, Harrison S, Shih J, Martinelli M (1997) Preclinical antitumor activity of cryptophycin-52/55 (C-52, C-55) against mouse tumors. Proc Am Assoc Cancer Res 38:225
13. Polin L, Valeriote F, Moore R, Tius M, Barrow R, Hemscheidt T, Liang J, Paik S, White K, Harrison S, Shih J, Martinelli M, Corbett T (1997) Preclinical antitumor activity of cryptophycin-52/55 (C-52, C-55) against human tumors in SCID mice. Proc Am Assoc Cancer Res 38:225
14. Corbett TH, Polin L, Roberts BJ, Lawson AJ, Leopold WR III, White K, Kushner J, Paluch J, Hazeldine S, Moore R, Rake J, Horwitz JP (2002) Transplantable syngeneic rodent tumors: solid tumors of mice. In: Teicher B (ed) Tumor models in cancer research. Humana Press, Totowa, pp 41–71
15. Corbett T, Valeriote F, LoRusso P, Polin L, Panchapor C, Pugh S, White K, Knight J, Demchik L, Jones J, Jones L, Lowichik N, Biernat L, Foster B, Wozniak A, Lisow L, Valdivieso M, Baker L, Leopold W, Sebolt J, Bissery M-C, Mattes K, Dzubow J, Rake J, Perni R, Wentland M, Coughlin S, Shaw JM, Liverside G, Liversidge E, Bruno J, Sarpotdar P, Moore R, Patterson G (1995) Tumor models and the discovery and secondary evaluation of solid tumor active agents. Int J Pharmacognosy [Suppl] 33:102–122
16. Foster BJ, Fortuna M, Media J, Wiegand RA, Valeriote FA (1998) Cryptophycin 1 cellular levels and effects in vitro using L1210 cells. Invest New Drugs 16:199–204
17. Noe DA (1998) Noncompartmental pharmacokinetic analysis. In: Grochow LB, Ames MM (eds) A clinician's guide to chemotherapy pharmacokinetics and pharmacodynamics. Lippincott, Williams & Wilkins, Baltimore, pp 515–530
18. Schultz RM, Shih C, Wood PG, Harrison SD, Ehlhardt WJ (1998) Binding of the epoxide cryptophycin analog, LY355703 to albumin and its effect on in vitro antiproliferative activity. Oncol Rep 5:1089–1094
19. Kessel D (1999) Protein-binding patterns of the antitumor antibiotic cryptophycin 52 as measured with a two-phase partitioning system. J Chromatogr B Biomed Sci Appl 735:121–126
20. Gerweck LE (2000) The pH difference between tumor and normal tissue offers a tumor specific target for the treatment of cancer. Drug Resist Updat 3:49–50